energies

MDPI

Article

Impact Identification of Carbon-Containing Carboniferous Clays on Surfaces of Friction Nodes

Iwona Jonczy [1,*], Andrzej Wieczorek [1], Krzysztof Filipowicz [1], Kamil Mucha [2], Mariusz Kuczaj [1], Arkadiusz Pawlikowski [1], Paweł Nuckowski [3] and Edward Pieczora [4]

[1] Faculty of Mining, Safety Engineering and Industrial Automation, Silesian University of Technology, Akademicka 2 Street, 44-100 Gliwice, Poland; andrzej.n.wieczorek@polsl.pl (A.W.); krzysztof.filipowicz@polsl.pl (K.F.); mariusz.kuczaj@polsl.pl (M.K.); arkadiusz.pawlikowski@polsl.pl (A.P.)
[2] Faculty of Mechanical Engineering and Robotics, AGH University of Science and Technology, Mickiewicza 30 Street, 30-059 Kraków, Poland; kmucha@agh.edu.pl
[3] Faculty of Mechanical Engineering, Silesian University of Technology, Konarskiego 18A Street, 44-100 Gliwice, Poland; pawel.nuckowski@polsl.pl
[4] KOMAG Institute of Mining Technology, Pszczyńska 37 Street, 44-100 Gliwice, Poland; epieczora@komag.eu
* Correspondence: iwona.jonczy@polsl.pl

Abstract: The article deals with issues related to the processes occurring in the wear result of steel surfaces of machine components in the presence of mineral grains. This type of destruction of cooperating surfaces usually takes place during the development of roadways or during mining of coal with use of longwall methods. Wear tests were carried out using the author's ring-on-ring test stand, on which the conditions of real wear of machine components in the presence of rocks were simulated. An abrasive material based on clayey rocks with an admixture of carbonaceous substance was used in the tests. Based on the analyses, it was found that the obtained results related to the damages are typical for wear mechanisms: microcracking and low-cycle fatigue. On the surface of the steel samples, numerous effects of micro-cutting and chipping could be observed, which were the result of the clayey impact of wear products and grains of the mineral substance. Under friction, a part of the abrasive and the carbon substance were pressed into generated microcracks, which is directly related to their plastic properties. The remaining, unpressed part of the abrasive material was subjected to further friction effects caused by the pressure of the tester pocket load and the relative movement of both steel rings surfaces. After the friction tests, the mixture of silty carbon abrasive material was in the form of flat aggregates on the samples' surfaces.

Keywords: claystone; clayey minerals; hard coal; friction; wear processes

Citation: Jonczy, I.; Wieczorek, A.; Filipowicz, K.; Mucha, K.; Kuczaj, M.; Pawlikowski, A.; Nuckowski, P.; Pieczora, E. Impact Identification of Carbon-Containing Carboniferous Clays on Surfaces of Friction Nodes. *Energies* **2021**, *14*, 1422. https://doi.org/10.3390/en14051422

Academic Editors: Dariusz Prostański and Sheng-Qi Yang

Received: 12 February 2021
Accepted: 2 March 2021
Published: 5 March 2021

1. Introduction

The properties of rocks are one of the key aspects to be taken into account during the development of roadways. Roadways separate an opened-up deposit, creating sections called mining panels, and are used for the run-of-mine haulage, supply of materials, air supply and personnel's movement. The mineral composition and petrographic features of the rocks through which the developed roadways pass, as well as the related physical and mechanical properties, are used to determine a selection of appropriate parameters of the equipment used for rock cutting [1].

The problem of excessive wear of steel surfaces of components such as flight bar conveyors is particularly important [2]. A flight bar conveyor is a haulage device in which transverse parts called scrapers are attached to a chain, continuously moving the run-of-mine to a specific location. It is intended for short-distance haulage of the run-of-mine in roadways and longwall coal, stone coal and stone workings. In mining conditions, flight bar conveyors, and their friction nodes in particular, are exposed to the impact of environmental conditions (e.g., mineral abrasives and mine water) and operational factors

(e.g., variable dynamic forces), which accelerate destructive processes [3,4]. The mechanism of surface destruction of metal parts depends on the given combination of the type of steel and mineral abrasive, as shown by Wieczorek [5].

Among the sedimentary rocks accompanying coal seams, the dominant group are clayey rocks represented by claystone—compact rocks with a massive texture, mostly made of clayey minerals, the grain size of which is below 0.01 mm. Zhang et al. [6] indicate the presence of three basic groups of ingredients in the composition of claystone: clay matrix, a composite matrix of clay and small mineral grains as well as imbedded quartz grains. The small size of clay minerals and their unique crystal structures give clay rocks some special properties, such as cation exchange capabilities, plastic behavior when wet, catalytic abilities, swelling behavior and low permeability [7,8].

Often, in shoals of clayey rocks, their stratification and susceptibility to breakdown into thicker or thinner plates compatible with sedimentation or pressure planes revealed during crushing can be observed. These types of rocks are commonly called shale clay (although their genesis is not related to metamorphism processes); they are formed as a result of late diagenesis processes. According to the Polish classification standards, among the Carboniferous rocks accompanying coal seams, there are also carbon clay and carbon shale—analogous to the rocks described above, with the difference that they contain admixtures of carbon substance. In carbon clay, the carbon substance is dispersed, forming a so-called pigment, while in carbon shale, it creates layers alternating with layers of clayey minerals. Ewy et al. [9] and Yu et al. [10], in their work, describe the formation of carbon shales, pointing to the loss of porosity and tighter compacting of the grains, which also cause a systematic change in their mechanical properties. They also point out that this type of clayey rock can crumble or show plastic properties. Similar studies were also conducted by Zhang et al. [11], pointing to the anisotropic nature of clayey rocks' properties, showing stratification. Liu et al. [12], in turn, indicated the possibility of creeping of clay rocks under the conditions of triaxial compression.

The correlations between clayey minerals and mechanical properties of claystone were studied by many scientists, but the impact of the type of clayey mineral on the mechanical properties of rocks is still poorly understood [13–17]. Authors of scientific papers often focus on studies concerning the properties of claystone subjected to high temperature [18,19], to verify the possibilities of using claystone in the ceramic industry; however, the behavior of clayey rocks under friction conditions and their impact on wear processes of steel components of machines are treated as a collateral.

Abrasive wear is one of the most common types of tribological wear, which can be defined as the process of destroying and removing material from the friction surface of a solid matter, accompanied by a change in mass, dimensions and shapes as well as the structure and physical properties of the rubbing parts [20,21]. The mechanism of this process, related to micro-scratching and micro-grooving, depends not only on the hardness of the worn surface but also on the type of abrasive material that affects it and, more precisely—on the hardness of the minerals contained in the abrasive material [22,23].

Micro-scratching, which causes significant surface degradation, is the main mechanism of friction damage in the case of hard abrasives such as quartz. The situation is different as regards abrasive materials made of soft rocks, where other wear mechanisms may occur, such as surface fatigue [24,25]. This type of process was noted during hard coal tests, which, like claystone, show plastic properties [26].

The results of studies on Carboniferous claystone subjected to friction in terms of its mineralogical and petrographic properties are presented in this article.

The main purpose of the study was to characterize the wear mechanisms in the presence of abrasives, based on clayey minerals and hard coal.

2. Material for Testing

Three types of clayey rocks taken from underground mining workings of three hard coal mines, located in the towns of Katowice, Jaworzno and Libiąż, within the Upper Silesian Coal Basin (South of Poland) (Figure 1), were subject to tests.

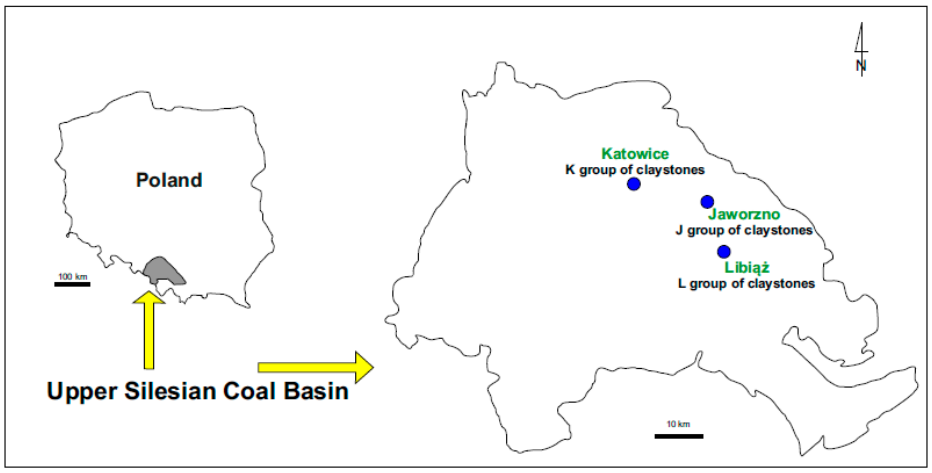

Figure 1. Schematic map of the Upper Silesian Coal Basin. The places from which samples were taken are marked.

The Upper Silesian Coal Basin is a triangular basin filled with Upper Carboniferous deposits; its area is about 6100 km^2, of which 1600 km^2 are located on the Czech side, forming the Ostrava-Karviná Basin. It is an orogenic basin, formed in the pre-mountain basin of the Moravian-Silesian Varyicide fold zone, with paralic and limnic formations. The carbon-bearing zone occurs at various depths—in the eastern part, down to a depth of 2400 m, and in the west, down to 4600 m—but the drilling shows that it can go even deeper, even down to 6000 m. Claystone occupies a significant position among the rocks accompanying coal seams [27,28].

3. Testing Methodology

Before the laboratory tests, some of the claystone samples were ground in a Retsch planetary ball mill with a tungsten carbide-lined vessel and then sieved through a 0.01-mm mesh screen. A fraction below 0.01 mm was used for phase identification by X-ray diffraction, chemical composition analysis and wear tests.

The specimens for microscopic examinations in transmitted light (thin plates) were prepared from broken-up claystone samples.

The laboratory tests included:

- A microscopic observation in thin plates of claystone, in transmitted light;
- A phase identification by X-ray diffraction (XRD);
- An analysis of the chemical composition of the claystone using the wavelength dispersive X-ray fluorescence method (WD-XRF);
- Wear tests;
- Microscopic observations using scanning electron microscopy of the surface of steel ring specimens after the wear tests.

Microscopic observations were carried out in transmitted light, in thin plates, using the OPTA-TECH LAB-40 HAL polarization diagnostic microscope made by OPTA-TECH, equipped with an image analyzer.

The phase composition tests were carried out in the X'Pert PRO MPD X-ray diffractometer made by Panalytical, equipped with a cobalt anode X-ray tube ($\lambda K\alpha$ = 0.179 nm) and a PIXcel 3D detector. Diffractograms were recorded in Bragg–Brentano geometry at the angle range of 5–100° 2Theta with a step of 0.026°, and the counting time per step was equal to 80 s. The HighScore Plus software (v. 3.0e) and the dedicated PAN-ICSD

(Inorganic Crystal Structure Database) database of inorganic crystal structures were used for the X-ray qualitative phase analysis.

The chemical composition of the samples was determined by the X-ray fluorescence method (WD-XRF) using the WD-XRF ZSX Primus II Rigaku spectrometer (Rh lamp). A qualitative spectrum analysis was performed by identifying the spectral lines and determining their possible coincidences. On this basis, analytical lines were selected. Semi-quantitative analysis was developed using the SQX Calculation software (fundamental parameters method). The analysis was carried out in the range of fluorine-uranium (F-U), and the content of the determined elements was normalized to 100%.

Wear tests were carried out for claystone samples using the author's test stand design (Section 4.2).

Observations of the samples' surfaces were carried out using the Supra 35 ZEISS scanning electron microscope with the detection of secondary electrons (SE) at an accelerating voltage of 20 kV and at magnification in the range of 60 ÷ 1000x. Qualitative analysis of the chemical composition in the micro-areas of the tested material was conducted using the characteristic X-ray energy spectroscopy (EDS) method at an accelerating voltage of 20 kV. The samples were sprayed with a thin layer of gold prior to testing to ensure the discharge of electric charge during testing.

4. Test Results

Laboratory tests were carried out in two stages: the first stage was related to the mineralogical and petrographic characteristics of claystone, and the second one to the wear tests.

4.1. Mineralogical and Petrographic Characteristics of Claystone

Claystone is characterized by its color, from light to dark grey, due to the presence of dispersed (in a form of a pigment) carbonaceous substance. The structure of the claystone is pellet and its texture is dense and generally chaotic, although in some samples of claystone, a stratification could be observed, which was reflected in dividing the rock into plates of several centimeters in thickness. Claystone becomes soft in the presence of water.

Microscopic observations of thin plates showed that their composition was dominated by clayey minerals, apart from which the presence of quartz and muscovite was also found (Figure 2).

Clayey minerals in the microscopic images form microcrystalline, colorless grains, with parallel polarizers showing grey interference colors of the first order. Quartz occurs in the form of colorless, generally allomorphic individuals with sharp-edged crumbs next to them; similarly to clayey minerals, it has the first-order interference colors. Muscovite creates elongated, automorphic grains with third-order interference colors. In some samples of the claystone, the characteristic presence of muscovite draws attention, where the elongated grains are arranged perpendicularly to the direction of the pressure impact, giving directional features to the rock texture (Figure 2c).

All the tested claystone samples contained a carbonaceous substance. The way of its occurrence was quite varied; in addition to the pigment being in a dispersed form, one can observe carbon crumbs of various sizes and elongated shapes in the form of laminates, which also give a directional feature to the claystone.

X-ray qualitative phase analysis showed that the clayey minerals group was represented by kaolinite $Al_4[Si_4O_{10}](OH)_8$ phase with an anorthic crystal structure ((Inorganic Crystal Structure Database): 98-003-1135). Diffraction lines from SiO_2 quartz with a hexagonal crystal lattice ((Inorganic Crystal Structure Database): 98-016-8354) and muscovite $KAl_2(OH,F)_2AlSi_3O_{10}$ with a monoclinic structure ((Inorganic Crystal Structure Database): 98-007-7497) were also identified on the diffractograms of all the tested claystone samples during microscopic observations in thin plates (Figure 3; Table 1).

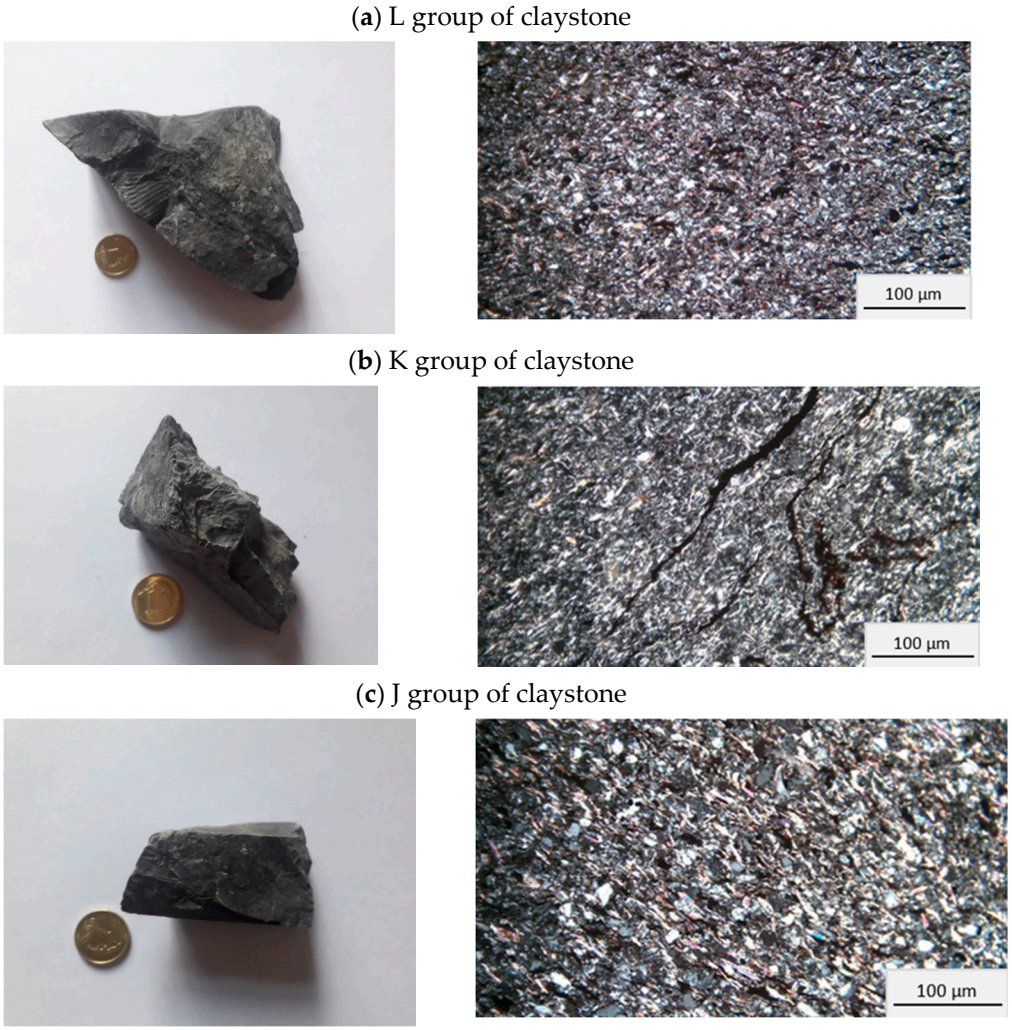

Figure 2. Claystone samples: left—macroscopic image; right—micro-photos in thin plates; crossed polarizers, magnification 100×.

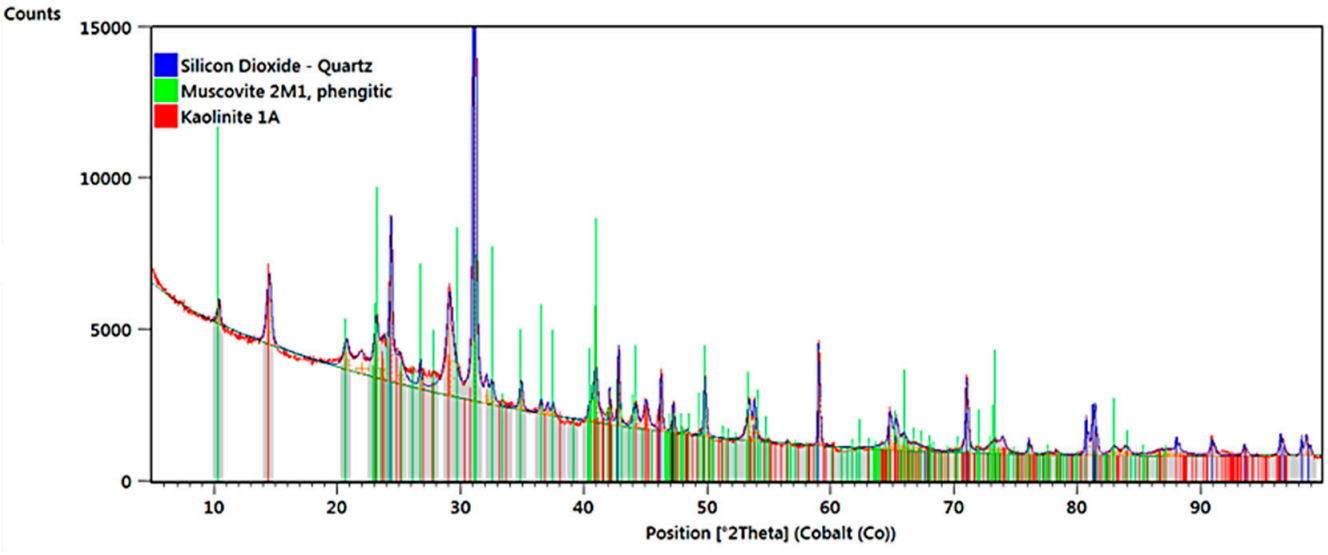

Figure 3. Diffractogram of the L group of claystone.

Table 1. Results of the claystone X-ray diffraction.

Pos. (°2Th.)	d-Spacing (Å)	Height (cts)	Compound	(h k l)
10.41	9.86	583	Muscovite 2M1	(0 0 2)
14.47	7.10	1580	Kaolinite 1A	(0 0 1)
20.74	4.97	613	Muscovite 2M1	(0 0 4)
23.16	4.45	1195	Muscovite 2M1	(1 1 −1)
23.76	4.34	702	Kaolinite 1A	(1 0 0)
24.35	4.24	3554	Silicon Dioxide	(0 1 0)
25.11	4.11	584	Muscovite 2M1	(0 2 −2)
26.73	3.87	686	Muscovite 2M1	(1 1 −3)
29.13	3.56	2258	Kaolinite 1A	(0 0 2)
31.12	.3.33	19,739	Silicon Dioxide	(0 1 1)
32.54	3.19	477	Muscovite 2M1	(1 1 4)
34.89	2.98	684	Muscovite 2M1	(0 2 −5)
36.52	2.85	346	Muscovite 2M1	(1 1 5)
37.47	2.78	307	Muscovite 2M1	(1 1 −6)
40.43	2.58	302	Muscovite 2M1	(1 3 −1)
41.03	2.56	653	Muscovite 2M1	(1 3 −2)
42.09	2.49	1141	Muscovite 2M1	(0 0 8)
42.79	2.45	2164	Silicon Dioxide	(1 1 0)
44.16	2.38	533	Muscovite 2M1	(1 3 3)
45.03	2.33	660	Kaolinite 1A	(2 1 2)
46.24	2.28	1495	Silicon Dioxide	(1 0 2)
47.23	2.23	851	Silicon Dioxide	(1 1 1)
49.80	2.12	1713	Muscovite 2M1	(1 3 5)
53.38	1.99	920	Muscovite 2M1	(0 0 10)
53.83	1.98	971	Silicon Dioxide	(2 0 1)
56.49	1.89	101	Kaolinite 1A	(1 2 3)
59.04	1.81	3187	Silicon Dioxide	(1 1 2)
64.80	1.67	856	Silicon Dioxide	(0 2 2)
65.32	1.66	606	Silicon Dioxide	(0 1 3)
65.89	1.64	248	Muscovite 2M1	(1 3 9)
71.01	1.54	2274	Silicon Dioxide	(1 2 1)
73.33	1.50	299	Muscovite 2M1	(3 3 −1)
73.96	1.49	257	Kaolinite 1A	(0 3 0)
76.08	1.45	476	Silicon Dioxide	(1 1 3)
78.30	1.42	115	Silicon Dioxide	(0 3 0)
80.73	1.38	1171	Silicon Dioxide	(1 2 2)
81.25	1.37	1513	Silicon Dioxide	(2 0 3)
81.46	1.37	861	Silicon Dioxide	(0 3 1)
82.93	1.35	199	Muscovite 2M1	(1 3 −13)
83.89	1.34	209	Muscovite 2M1	(2 0 12)
87.23	1.30	148	Muscovite 2M1	(2 6 0)
88.05	1.29	453	Silicon Dioxide	(1 0 4)
90.90	1.25	444	Silicon Dioxide	(3 0 2)
93.52	1.23	338	Silicon Dioxide	(2 2 0)
96.49	1.20	668	Silicon Dioxide	(2 1 3)
98.20	1.18	505	Silicon Dioxide	(1 1 4)
98.62	1.17	595	Silicon Dioxide	(1 3 0)

In all the tested claystone groups, the chemical composition was similar (Table 2).

Silica (SiO_2) was the dominant component; its content ranged from 58.80% to 64.39%. The second most abundant compound in all the tested samples was Al_2O_3; its content ranged from 27.90% to 29.05%. The presence of silica and alumina is mainly related to the presence of silicate minerals: quartz, kaolinite and muscovite. Subsequently, in claystone, the following oxides are associated with the presence of aluminosilicates: K_2O (2.95–3.99%), Fe_2O_3O (0.98–3.85%), TiO_2 (1.25–1.39%) and MgO (0.56–1.51%). The remaining compounds are present in smaller amounts; in general, their content does not exceed 1%.

Table 2. Results of the claystone chemical analysis.

Marking	Content (% Weight)		
	L Group of Claystones	K Group of Claystones	J Group of Claystones
Na_2O	0.74	0.49	0.26
MgO	1.51	0.99	0.56
Al_2O_3	27.90	28.07	29.05
SiO_2	58.80	62.47	64.39
P_2O_5	0.13	0.05	0.07
SO_3	0.66	0.18	0.15
Cl	0.62	0.11	0.03
K_2O	3.99	3.78	2.95
CaO	0.18	0.05	0.12
TiO_2	1.30	1.39	1.25
V_2O_5	0.04	-	0.02
Cr_2O_3	0.03	0.03	0.01
MnO	0.04	0.02	0.01
Fe_2O_3	3.85	2.05	0.98
Co_2O_3	-	0.003	-
NiO	0.01	0.008	0.01
CuO	0.01	0.006	0.004
ZnO	0.03	0.006	0.004
Ga_2O_3	0.005	0.005	0.006
Rb_2O	0.02	0.02	0.02
SrO	0.01	0.01	0.008
ZrO_2	0.06	0.06	0.06
BaO	0.07	0.20	0.06
PbO	0.006	0.005	-
Σ	100.011	100.003	100.022

4.2. Wear Tests

The author's ring-on-ring test stand was used to analyze the impact of friction conditions on the tested claystone samples (Figure 4). The conditions generated on the test stand simulated the conditions of the real wear of machine components in the presence of claystone.

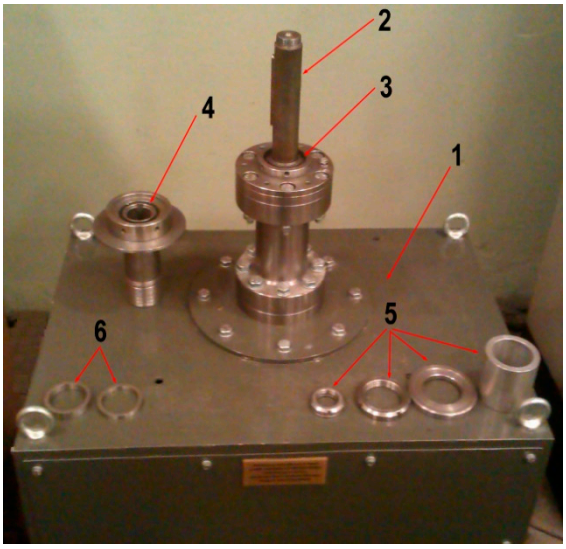

Figure 4. The design of the tribotester: 1—test stand body with a motor; 2—driving shaft; 3—upper holder of the sample; 4—bottom holder of the sample; 5—fixing components; 6—steel ring samples.

The presence, between the steel ring samples, of crushed abrasives grains and wear products from the damaged surface is a characteristic feature of the test stand. The main

friction pair consists of two ring steel samples of an external diameter of ø55 mm and an internal diameter of ø45 mm, between which there is an abrasive material (Figure 5). Ring samples, made of Hardox 400 wear-resistant steel of a surface hardness in the range 380 ÷ 405 HB, were used in the tests, consisting in turning and grinding.

Figure 5. Ring samples.

After each 10-min cycle of the wear test, the samples were cleaned, weighed and supplemented with fresh abrasive material in a volume of 1 cm^3. The test for each abrasive material consisted of eight 10-min cycles—each test was repeated three times. The basic wear test parameters are presented in Table 3.

Table 3. Basic parameters of the wear tests.

Parameter	Amount
Nominal unit pressure σ, MPa	0.125
Peripheral speed v, m/s	0.29
Time of testing, min	8 × 10
Sliding distance, m	1392

Loss of mass u_M, used to determine the frictional wear, was determined according to the following Formula (1):

$$u_M = \left(m_{pd0} - m_{pdt}\right) + \left(m_{pg0} - m_{pgt}\right) \quad (1)$$

where:

u_M—loss of the sample mass, g;
m_{pd0}—mass of the bottom sample before the test, g;
m_{pdt}—end mass of the bottom sample, g;
m_{pg0}—mass of the top sample before the test, g;
m_{pgt}—end mass of the top sample, g.

The uncertainty of mass wear determination was given for the significance level of 0.95 and the degree of freedom f = 4. Relative measurement uncertainty was less than 1% for all the considered cases. The test results are illustrated in the form of the diagrams presented below (Figure 6a,b). The greatest loss of mass was noted in the case of the claystone of group J, and the smallest for the claystone of group L (Figure 6a). These results correlate with the chemical composition of claystone; among all the tested rocks, the claystone of group J contained the highest amount of SiO_2 (64.39%), while in the claystone of group L,

the SiO_2 content was the lowest—58.80%. This relationship is also visible in Figure 6b—loss of mass increases with increasing SiO_2 and Al_2O_3 oxides content (Figure 6b).

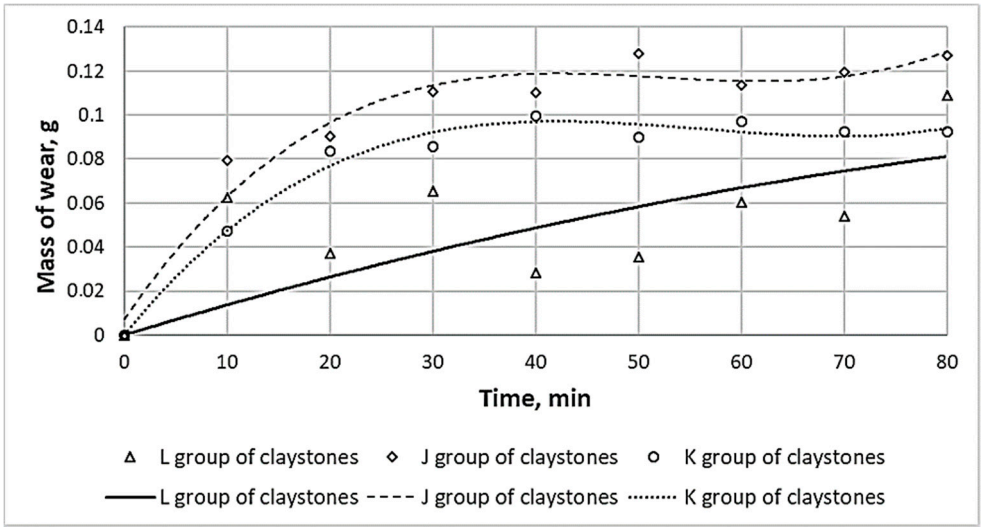

(**a**)

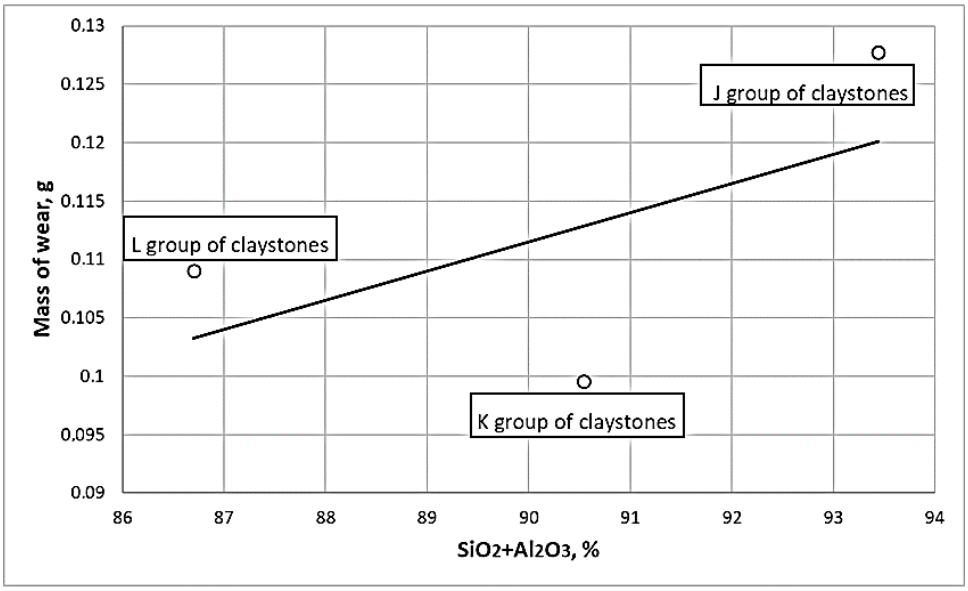

(**b**)

Figure 6. Wear diagram at maximum load (**a**) as a time curve; (**b**) in a function of chemical content.

An assessment of clayey abrasives' impact on the surface of the tested steel samples was the next stage of testing after the wear tests. For this purpose, sample surfaces were observed using scanning electron microscopy. On the surface of all the analyzed samples subjected to wear tests, scratches were observed, the presence of which was most likely caused by the impact of the products of the surface fatigue chipping process and partly by the oxides (SiO_2 and Al_2O_3), the grains of which could be aggregated under the load. It was found that due to the wear caused by the presence of the abrasive material between the cooperating surfaces, two main components of the abrasive, kaolinite and the carbon substance, were pressed into the formed scratches (Figures 7–10).

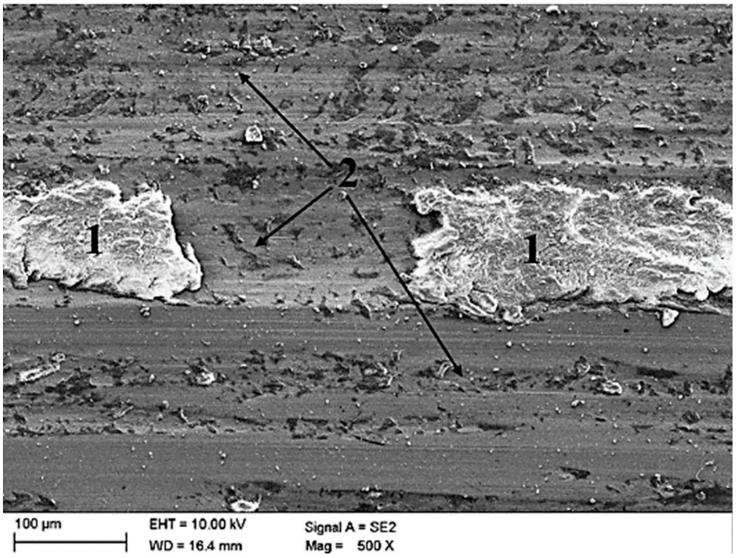

Figure 7. Steel sample surface after the wear tests; 1—kaolinite; 2—scratches.

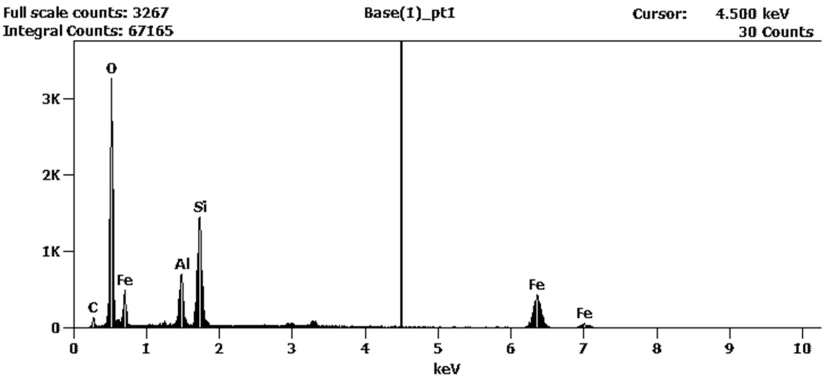

Figure 8. EDS of Point 1 according to Figure 7.

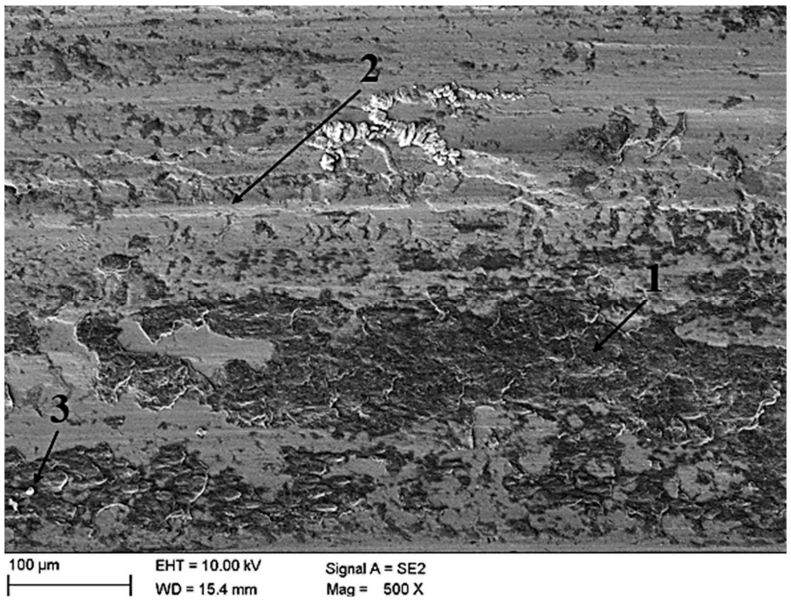

(**a**)

Figure 9. *Cont.*

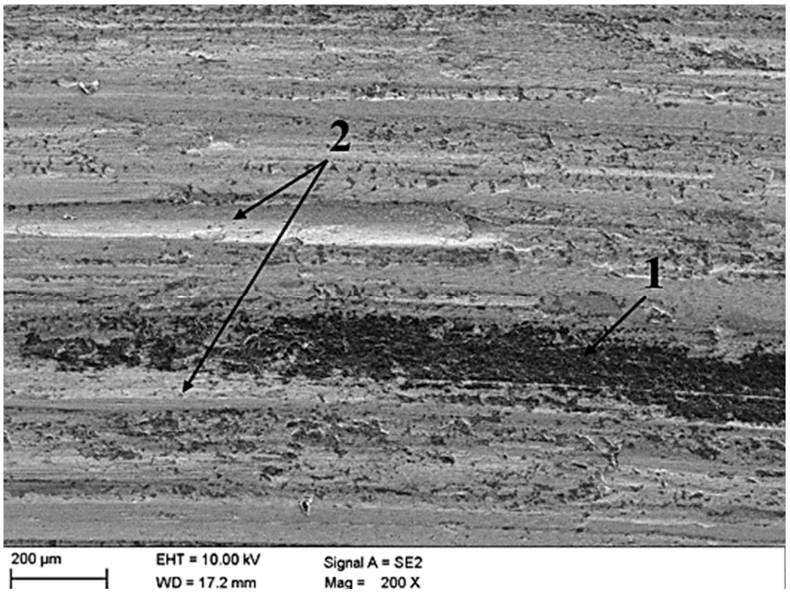

(**b**)

Figure 9. Steel sample surface after the wear tests; (**a**) 1—clayey abrasive with a carbon substance; 2—scratches; 3—a grain pressed into the clayey abrasives; (**b**) 1—clayey abrasive with a carbon substance; 2—scratches.

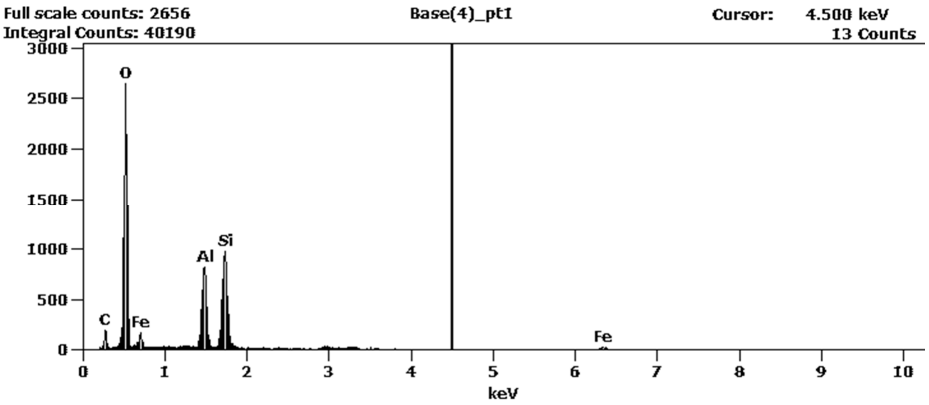

(**a**)

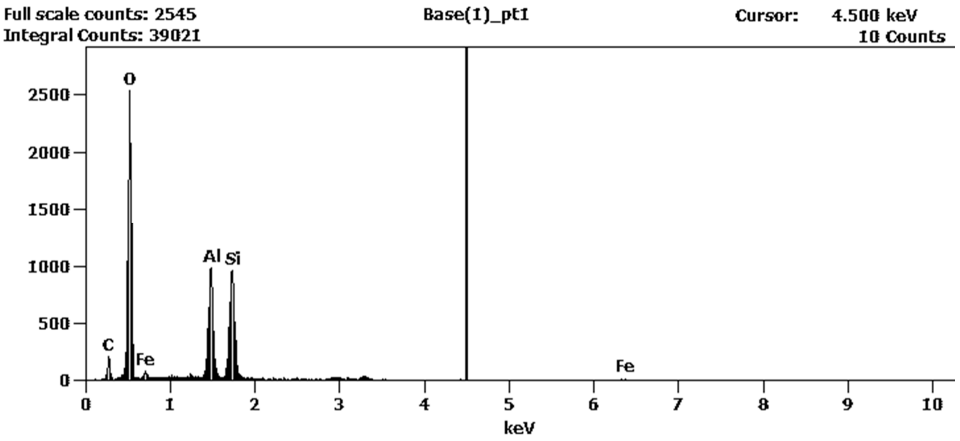

(**b**)

Figure 10. EDS spectrum of Point 1 according to Figure 9a (**a**); EDS spectrum of Point 1 according to Figure 9b (**b**).

The remaining unpressed part of the abrasive material was subject to friction. This abrasive, under the load and relative movement of the surface, tended to aggregate into larger aggregates of elongated shape, which were most often located in the areas of the surface chipping (Figures 11 and 12).

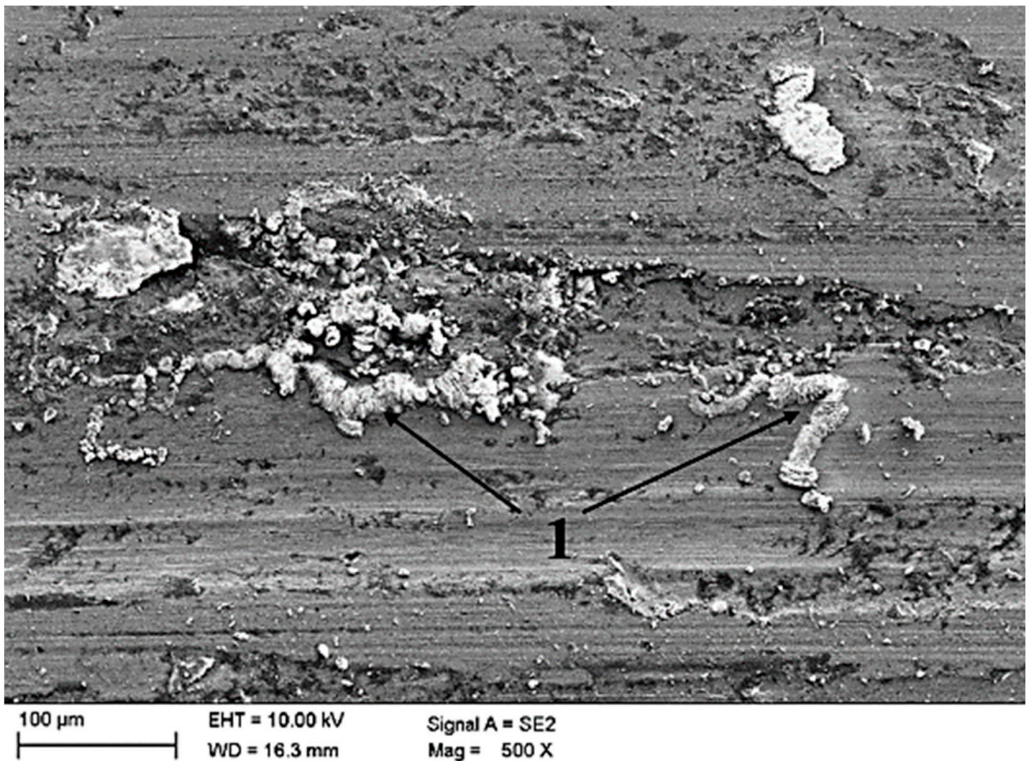

Figure 11. Steel sample surface after the wear tests; 1—aggregates of clay coal abrasive material.

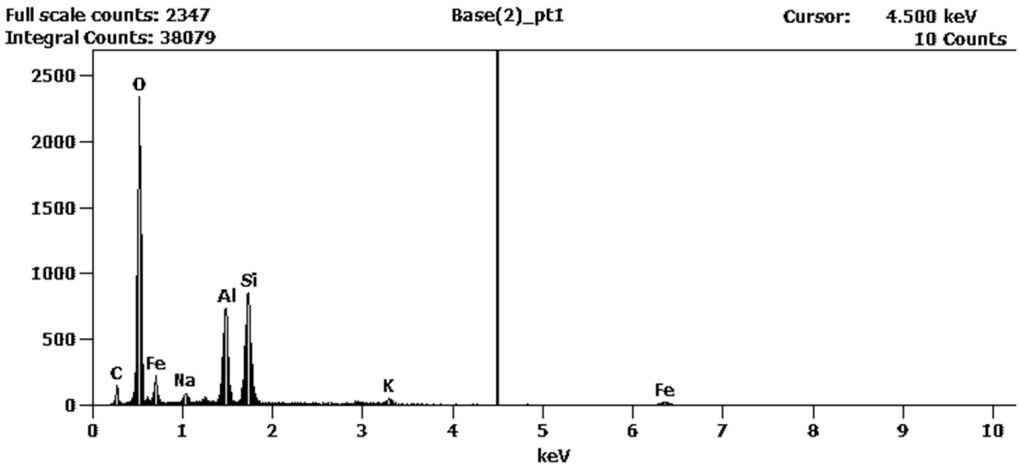

Figure 12. EDS spectrum of Point 1 according to Figure 11.

Damage to the top layer of the sample surface, in the form of scaly cracks, was observed (Figure 13), initiating flat, fatigue fracturing of the steel surface (Figure 14).

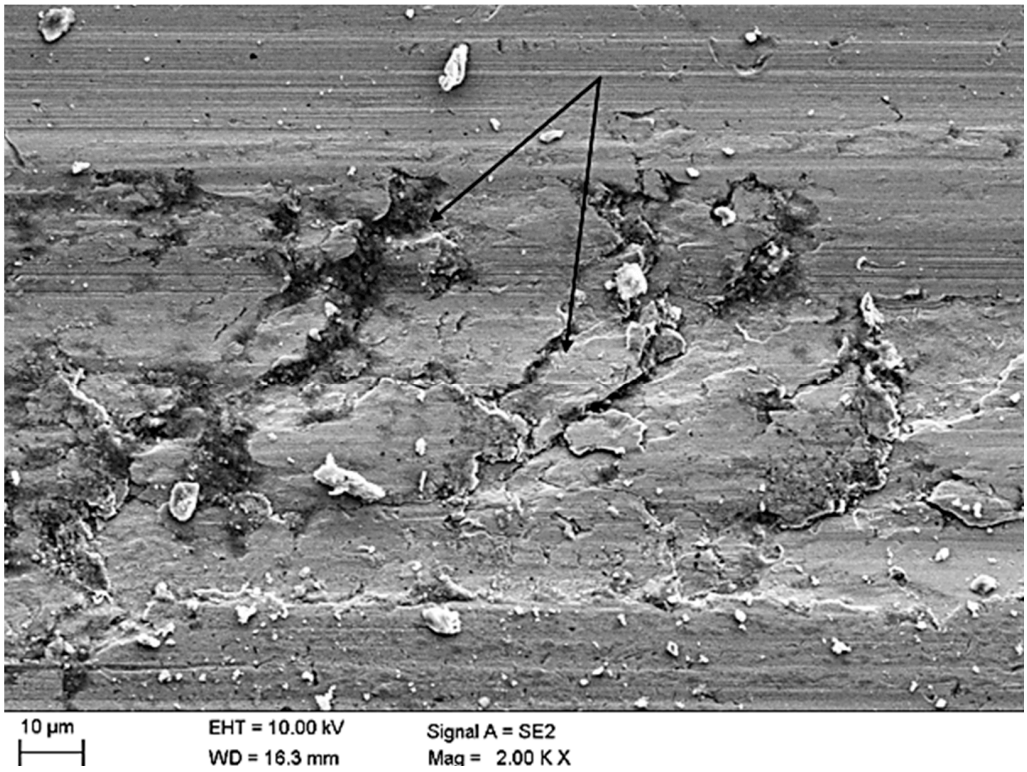

Figure 13. Steel sample surface worn as a result of the presence of clay coal abrasive material with visible surface cracks (indicated with arrows).

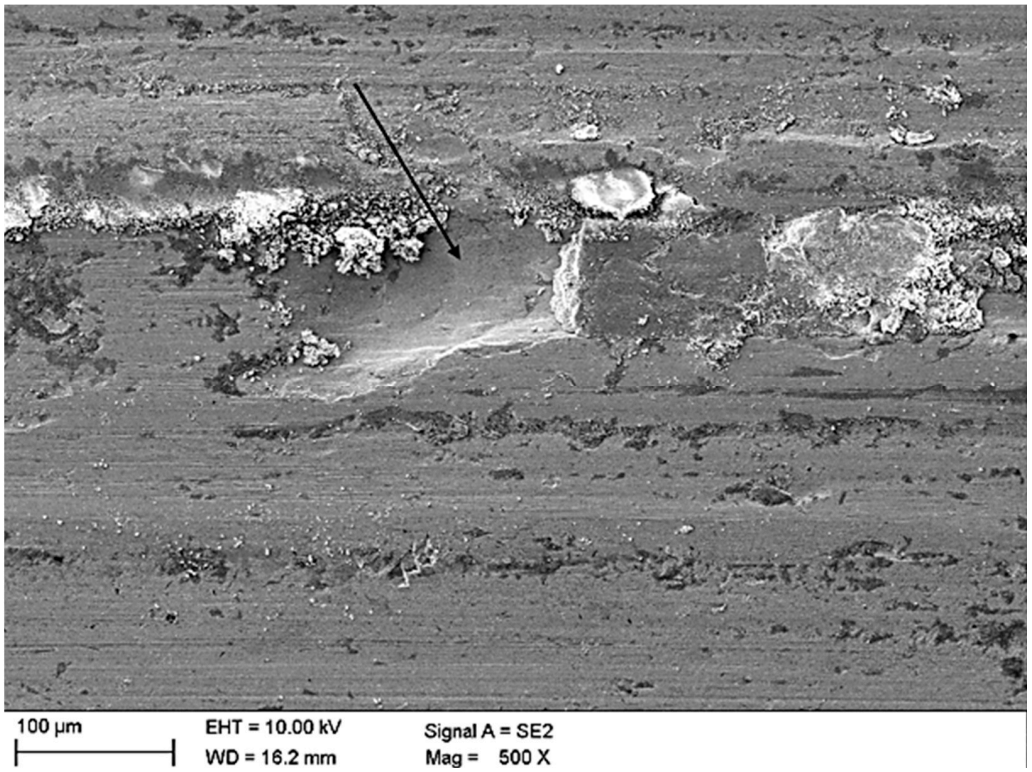

Figure 14. Steel sample surface worn as a result of the presence of clay coal abrasive material with visible surface chipping (indicated with arrows).

5. Discussion

The behavior of clayey rocks subject to friction is directly related to the properties of the clay minerals that form the rock. Their morphology in the form of thin plates as well as their arrangement enable the water, metal cations and particles of organic compounds (Figure 15) to enter the structure of clayey minerals.

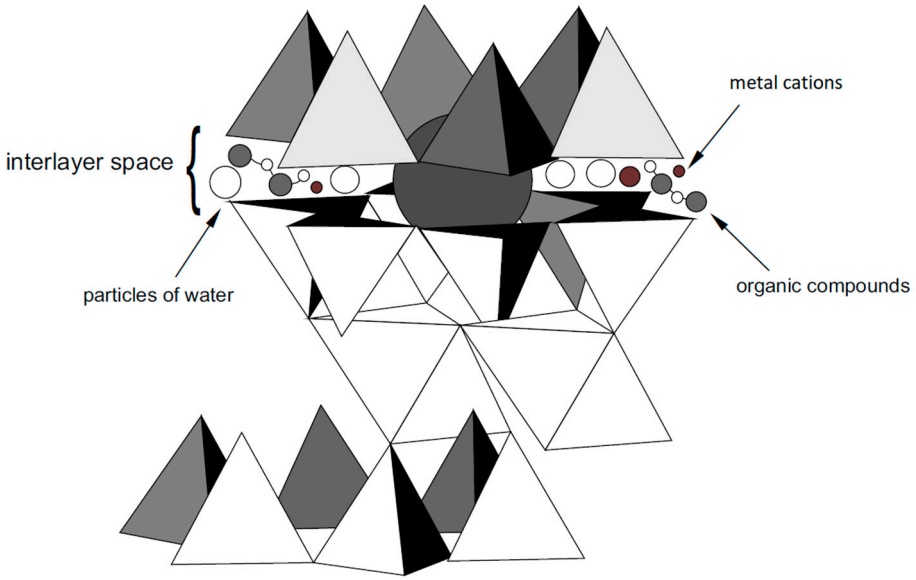

Figure 15. Modification scheme of the clay internal structure allowing sorption of heavy metals and organic compounds by K. Bahranowski, 2000 [29].

In the case of the tested claystone, the clayey minerals are represented by kaolinite, belonging to the group of two-layer minerals, where their packages are permanently bound by hydrogen bonds (hydrogen of octahedron OH groups). The bonds are so strong that they make an increase in the space between the packages impossible, thus preventing an ingress of water and additional cations. The carbonaceous substance, determined in the tested clayey rocks, is, therefore, a component that occurs simultaneously with the mineral phases. Plastic properties of both clayey minerals and carbonaceous substance were revealed during the wear tests.

The test results indicate that in the case of the tested claystone, the fatigue processes, related to the cyclical impact of contact stresses in the surface layers of the cooperating components, are the basic form of damage. This type of interaction leads to the formation of surface cracks that are formed during friction under the impact of repeated elastic–plastic or plastic deformations.

Cracks on the surface became visible under the impact of this type of abrasive material, which led to further delamination. The delamination wear process has been described by Fleming and Suh [30] and Stachowiak and Zwierzycki [31] as also Stachowiak and Stachowiak [32]. Each point of contact on the surface of the steel sample of the sliding node is cyclically loaded by the roughness of the abrasive particles. An accumulation of plastic deformations and stresses in the subsurface layer and cracks in the subsurface layer of the steel sample are the consequences of these interactions. The gaps that arise during further cyclical loading of the contact area can grow. The growth of such cracks is initially tangent to the friction surface and then propagates towards the surface. Separation of the subsurface layer in the form of a specific thin scale is the end result of the fatigue process.

Cracking of the surface layer under the impact of high pressure and micro-fatigue leads to the formation of wear products—steel particles, which can behave, in terms of wear, in the same way as hard mineral abrasives. As a result of the impact of crushed wear products as well as aggregated grains of the mineral substance, traces of micro-cutting were

observed on the surface of the tested steel samples, which should be treated as secondary damage in relation to the low-cycle fatigue wear of the steel surface layer.

During the tests, kaolinite as well as carbon particles present in claystone were partially pressed into the cracks. The mechanism of such a behavior is typical for plastic materials, which was proven by the authors during previous tests on the example of hard coal [26]. This process was also described by Pertica et al. [33] and Xia et al. [34], indicating the presence of a wear mechanism in the form of micro-fatigue. Due to the fact that low-hardness abrasive particles are not sharp enough or the steel surface has high strength and plasticity, the slip between them leads to their indentation in the unevenness and the gaps present on the surface of the steel component. At the place of pressing, a convexity is formed, which, under the impact of further loading with further particles, causes the formation of plastic deformations on the surface, which may lead to the formation of a crack [34].

The wear tests carried out on steel samples showed that with successive loads, the largest loss of total weight of the steel samples was found when using a claystone-based abrasive marked with the symbol J, and the smallest for the abrasive L of the clayey group. The test results correlate with the chemical composition of claystone (Table 1 and Figure 7b). Among all the tested rocks, the claystone of group J contained the highest amount of SiO_2 (64.39%), while in the claystone of group L, the SiO_2 content was the lowest—58.80%. Microscopic observations indicate that silica is associated with the presence of quartz, a significant amount of which was determined in thin plates during microscopic observations in all the analyzed samples. Aggregated quartz grains can form abrasive grains, causing a destruction of the top layer of steel samples by the formation of cracks, thus causing losses in the material [35,36]. These losses can have a different morphology. During wear tests, Stachowiak and Stachowiak [31] found that rounded grains of abrasive minerals form round craters and smooth grooves, while angular ones form sharp indentations and narrow cutting grooves.

In general, it should be stated that the wear in the presence of ground clayey particles was not intensive. This could be explained by the plastic properties of clayey minerals, enabling them to be pressed into the primary cracks formed at the stage of making samples during grinding and secondary ones, i.e., fatigue chipping and cuts caused by the crushed steel (wear products). A compacted clayey material formed in this way could protect the surface formed after a detachment of the chipping from oxidation. At the same time, the claystone layer formed as a result of friction and transferred compressive and tangential stresses related to the relative movement of the samples, which was the direct cause of steel fatigue chipping. It is also likely that the chippings and mineral aggregates were partially inactivated by a layer of compressed clay abrasive (Figure 10 shows particles embedded in the clayey material).

6. Conclusions

Based on the tests, it has been concluded that kaolinite, quartz and muscovite dominate in the mineral composition of the examined clayey rocks. In all the tested samples, the presence of carbonaceous substance was found, which occurred in various forms: as a pigment and in the form of crumbs of various sizes as well as a small lamination.

The chemical composition of rocks is closely related to the chemical composition of the minerals that build them, and the dominant ingredients are the following ones: SiO_2, Al_2O_3 as well as K_2O, Fe_2O_3, TiO_2 and MgO.

In the wear tests using the abrasives, based on clayey minerals and hard coal, the effects of the wear processes were manifested in damage typical for wear mechanisms: micro-scratching and micro-fatigue.

Under the action of wear products and quartz on the surface of the steel samples, cracks were visible, which led to delamination. During the wear tests, kaolinite and a carbonaceous substance were pressed into the cracks due to the plastic properties of both clayey minerals and coal.

The grains of crushed chippings and mineral aggregates could be partially inactivated by a layer pressed in claystone.

Author Contributions: Conceptualization, I.J. and A.W.; methodology, A.W. and K.F.; experimental studies, I.J., A.W., P.N. and K.M.; simulation studies, M.K.; formal analysis, M.K. and A.P.; investigation, P.N. and A.P.; resources, E.P. and K.M.; data curation, I.J. and A.W.; writing—original draft preparation, I.J., A.W. and K.M.; writing—review and editing, E.P.; visualization, A.P.; funding acquisition, K.F. All authors have read and agreed to the published version of the manuscript.

Funding: The publication was created as part of BK-296/RG-2/2020, 06/020/BK_20/0046: Testing the resistance of the materials used in the components of roadway flight-bar conveyor to wear during action of rock abrasive materials.

Institutional Review Board Statement: Not applicable.

Informed Consent Statement: Not applicable.

Data Availability Statement: Not applicable.

Conflicts of Interest: The authors declare no conflict of interest.

References

1. Kotwica, K. Atypical and innovative tool, holder and mining head designed for roadheaders used to tunnel and gallery drilling in hard rock. *Tunn. Undergr. Space Technol.* **2018**, *82*, 493–503. [CrossRef]
2. Wang, S.; Ge, Q.; Wang, J. The impact wear-resistance enhancement mechanism of medium manganese steel and its applications in mining machines. *Wear* **2017**, *376–377*, 1097–1104.
3. Myszka, D.; Wieczorek, A.N. Effect of Phenomena Accompanying Wear in Dry Corundum Abrasive on the Properties and Microstructure of Austempered Ductile Iron with Different Chemical Composition. *Arch. Met. Mater.* **2015**, *60*, 483–490. [CrossRef]
4. Wieczorek, A.N. Operation-Oriented Studies on Wear Properties of Surface-Hardened Alloy Cast Steels Used in Mining in the Conditions of the Combined Action of Dynamic Forces and an Abrasive Material. *Arch. Met. Mater.* **2017**, *62*, 2381–2389. [CrossRef]
5. Wieczorek, A.N. Experimental studies on the influence of abrasive materials on the wear of hard-wearing steels. *Tribologia* **2018**, *49*, 133–141. [CrossRef]
6. Zhang, F.; Guo, H.; Hu, D.W.; Shao, J.-F. Characterization of the mechanical properties of a claystone by nano-indentation and homogenization. *Acta Geotech.* **2018**, *13*, 1395–1404. [CrossRef]
7. Barton, C.D.; Karathanasis, A.D. Clay minerals. In *Encyclopaedia of Soil Science*; Marcel Dekker: New York, NY, USA, 2002.
8. Aboudi Mana, S.C.; Hanafiah, M.M.; Chowdhury, A.J.K. Environmental characteristics of clay and clay-based minerals. *J. Geol. Ecol. Landsc.* **2017**, *1*, 155–161. [CrossRef]
9. Ewy, R.; Dirkzwager, J.; Bovberg, C. Claystone porosity and mechanical behavior vs. geologic burial stress. *Mar. Pet. Geol.* **2020**, *121*, 104563. [CrossRef]
10. Yu, C.Y.; Chow, J.K.; Wang, Y.-H. Pore-size changes and responses of kaolinite with different structures subject to consolidation and shearing. *Eng. Geol.* **2016**, *202*, 122–131. [CrossRef]
11. Zhang, F.; Xie, S.Y.; Hu, D.W.; Shao, J.F.; Gatmiri, B. Effect of water content and structural anisotropy on mechanical property of claystone. *Appl. Clay Sci.* **2012**, *69*, 79–86. [CrossRef]
12. Liu, Z.; Shao, J.; Xie, S.; Conil, N.; Zha, W. Effects of relative humidity and mineral compositions on creep deformation and failure of a claystone under compression. *Int. J. Rock Mech. Min. Sci.* **2018**, *103*, 68–76. [CrossRef]
13. Supandi, S.; Zakaria, Z.; Sukiyah, E.; Sudradjat, A. The correlation of exposure time and claystone properties at the Warukin Formation Indonesia. *Int. J. Geomate* **2018**, *15*, 188–195. [CrossRef]
14. Supandi, S.; Zakaria, Z.; Sukiyah, E.; Sudradjat, A. The Influence of Kaolinite—Illite toward mechanical properties of Claystone. *Open Geosci.* **2019**, *11*, 440–446. [CrossRef]
15. Plé, O.; Manicacci, A.; Gourc, J.-P.; Camp, S. Flexural behavior of a clay layer: Experimental and numerical study. *Can. Geotech. J.* **2012**, *49*, 485–493. [CrossRef]
16. Tiwari, B.; Marui, H. Influences of clay mineralogy in residual shear strength of soil. *Ann. Rep. Res. Inst. Hazards Snowy Areas Niigata Univ.* **2002**, *24*, 37–56.
17. Mucha, K. The new method for assessing rock abrasivity in terms of wear of conical picks. *New Trends Prod. Eng.* **2019**, *2*, 186–194. [CrossRef]
18. Hettema, M.H.H.; Niepce, D.V.; Wolf, K.H.A.A. A microstructural analysis of the compaction of claystone aggregates at high temperatures. *Int. J. Rock Mech. Min. Sci.* **1999**, *36*, 57–68. [CrossRef]
19. Tian, H.; Ziegler, M.; Kempka, T. Physical and mechanical behavior of claystone exposed to temperatures up to 1000 °C. *Int. J. Rock Mech. Min. Sci.* **2014**, *70*, 144–153. [CrossRef]

20. Scott, D. Wear. In *Industrial Tribology—The Practical Aspects of Friction, Lubrication and Wear*; Elsevier: Amsterdam, The Netherlands, 1983; pp. 12–30.
21. Hawk, J.A.; Wilson, R.D. Tribology of Earthmoving, Mining, and Minerals Processing. In *Modern Tribology Handbook*; Bhushan, B., Ed.; CRC Press LLC.: Boca Raton, FL, USA, 2001; Volume 35.
22. Yaralı, O.; Yaşar, E.; Bacak, G.; Ranjith, P.G. A study of rock abrasivity and tool wear in Coal Measures Rocks. *Int. J. Coal Geol.* **2008**, *74*, 53–66. [CrossRef]
23. Terva, J.; Teeri, T.; Kuokkala, V.-T.; Siitonen, P.; Liimatainen, J. Abrasive wear of steel against gravel with different rock–steel combinations. *Wear* **2009**, *267*, 1821–1831. [CrossRef]
24. Zum Gahr, K.H. *Microstructure and Wear of Materials*; Tribology Series; Elsevier: Amsterdam, The Netherlands, 1987.
25. Tylczak, J.H. Abrasive wear. In *ASM Handbook Vol. 18. Friction, Lubrication, and Wear Technology*; ASM International: Almere, The Netherlands, 1992; pp. 184–190.
26. Jonczy, I.; Wieczorek, A.N.; Podwórny, J.; Gerle, A.; Staszuk, M.; Szweblik, J. Characteristics of hard coal and its mixtures with water subjected to friction. *Gospod. Surowcami Miner. Miner. Resour. Manag.* **2020**, *36*, 185–201.
27. Polish Geological Institute—National Research Institute. Mineral Resources of Poland: Hard Coal. General Information and Occurrence. Available online: http://geoportal.pgi.gov.pl/surowce/energetyczne/wegiel_kamienny/2019 (accessed on 31 October 2020).
28. Polish Geological Institute—National Research Institute. Geology of the Upper Silesia Coal Basin. Available online: http://geoportal.pgi.gov.pl/zrozumiec_ziemie/wycieczki/jura_krakowsko_czestochowska_1#001 (accessed on 31 October 2020).
29. Ratajczak, T.; Hycnar, E.; Bożęcki, P. Kryterium mineralogiczne jako element oceny przydatności niektórych polskich surowców ilastych do budowy przesłon hydroizolacyjnych. Studia, Rozprawy, Monografie nr 194, Instytutu Gospodarki Surowcami Mineralnymi i Energią PAN, Kraków. 2015. Available online: https://min-pan.krakow.pl/wp-content/uploads/sites/4/2017/12/SRM-194.pdf (accessed on 4 February 2021).
30. Fleming, J.R.; Suh, N.P. Mechanics of crack propagation in delamination wear. *Wear* **1977**, *44*, 39–56. [CrossRef]
31. Stachowiak, A.; Zwierzycki, W. Zużycie delaminacyjne stali AISI 304 w warunkach tribokorozji. Delamination wear of steel AISI 304 in tribocorrosive conditions. *Tribologia* **2010**, *5*, 315–322.
32. Stachowiak, G.B.; Stachowiak, G.W. The effects of particle characteristics on three-body abrasive wear. *Wear* **2001**, *249*, 201–207. [CrossRef]
33. Petrica, M.; Peissl, S.; Badisch, E. Influence of Coal on the Wear Behavior of Steels in 3-Body Conditions. *Key Eng. Mater.* **2014**, *604*, 75–78. [CrossRef]
34. Xia, R.; Li, B.; Wang, X.; Yang, Z.; Liu, L. Screening the Main Factors Affecting the Wear of the Scraper Conveyor Chute Using the Plackett–Burman Method. *Math. Probl. Eng.* **2019**, *2019*, 1–11. [CrossRef]
35. Mutton, P.J. *Abrasion Resistant Materials for the Australian Minerals Industry*; Australian Minerals Industries Research Association Limited: Melbourne, Australia, 1988; Volume 1.
36. Ratia, V.; Heino, V.; Valtonen, K.; Vippola, M.; Kemppainen, A.; Siitonen, P.; Kuokkala, V.T. Effect of abrasive properties on the high-stress three-body abrasion of steels and hard metals. *Tribol. Finn. J. Tribol.* **2014**, *32*, 3–18.